Excitonic lifetime for double-barrier heterostructures in the presence of phonons

A. Hernández-Cabrera, P. Aceituno, and H. Cruz
Departamento de Física Fundamental y Experimental, Universidad de La Laguna, 38204 La Laguna, Tenerife, Spain
(Received 30 May 1995)

In this work, we have numerically integrated in space and time the effective-mass Schrödinger equation for an electron-hole pair in a GaAs/AlAs double-barrier heterostructure. Considering the electron-phonon interaction and an external electric field, we have studied the excitonic tunneling escape process from the double-barrier quantum well. In this way, electronic lifetimes have been obtained at different well widths and applied electric fields.

Since its discovery,[1] resonant tunneling through semiconductor heterostructures has been the object of great attention due to its possible applications to ultra-high-speed electronic devices.[2] With the development of such devices, it has become important to carry out theoretical and experimental studies on the tunneling process of carriers. One of the most important time-domain experiments in double-barrier heterostructures was realized by Tsuchiya, Matsusue, and Sakaki.[3] They studied the decay of an exciton localized between two barriers in a single quantum well using a technique of picosecond time-resolved photoluminescence. The experiment is schematically illustrated in Fig. 1. The incoming laser creates an electron-hole pair that is localized in the quantum-well region, and then its decay rate is determined by analyzing the time-resolved photoluminescence. They used a single-particle model to describe electron tunneling neglecting the existence of hole tunneling and excitonic effects. They found that the experimental data matched the calculated tunneling time in the case of sufficiently thin barriers.[3]

In the case of such a double-barrier system, it has been recently shown that if the applied electric field is large enough, the hole tunneling process becomes important. In this way, an excitonic wave function for the electron-hole pair will be needed to explain the carrier wave-packet dynamics.[4] With the use of an excitonic model for tunneling,[4] it was possible to explain in part the differences between theoretical and experimental results.[3] In addition to this, the electron-optical phonon coupling has been recently studied in the case of double barriers. It is found that the different phonon modes in the quantum well contribute significantly to the electronic tunneling escape process.[5] Taking this into account, in this work we will propose a calculation method to study the time-dependent evolution of excitonic electron-hole pairs considering an electron-optical phonon interaction. The calculation method will be based on the discretization of space and time for both carrier wave packets.

In order to study the dynamics of excitonic tunneling, we need to solve the time-dependent Schrödinger equation associated with the Hamiltonian for a spinless exciton in the heterostructure region. The excitonic Hamiltonian is given by[4]

$$H(\mathbf{r}_e,\mathbf{r}_h)=-\frac{\hbar^2}{2\mu_{xy}}\nabla^2_{xy}+\sum_{i=e,h}\left[-\frac{\hbar^2}{2m_i^*}\frac{\partial^2}{\partial z_i^2}+V_i(z_i)+H_{i\text{-ph}}\right]-\frac{e^2}{\epsilon\sqrt{\rho^2+(z_e-z_h)^2}}\ , \tag{1}$$

where the subscripts e,h refer to electrons or holes, respectively, and $V_e(z_e)$, $V_h(z_h)$ are the potentials due to the quantum wells. The term $H_{i\text{-ph}}$ represents the carrier-phonon interaction. The m_e^* and m_h^* values are the effective masses, μ_{xy} is the reduced x-y plane electron-hole mass, and $\rho=\rho_c-\rho_h$ is the relative motion within the quantum-well plane. The second term represents the Coulomb electron-hole potential.

In our model, the electron-phonon interaction can be described using second-order perturbation theory. In such a case, δE, δm^*, and $\delta\mu$ are the corrections to energy and effective masses, respectively. Taking this into account, we can write Eq. (1) as

$$H(\mathbf{r}_e,\mathbf{r}_h)=-\frac{\hbar^2}{2M_{xy}^*}\nabla^2_{xy}+\sum_{i=e,h}\left[-\frac{\hbar^2}{2M_i^*}\frac{\partial^2}{\partial z_i^2}+V_i(z_i)+\delta E_i\right]-\frac{e^2}{\epsilon\sqrt{\rho^2+(z_e-z_h)^2}}\ , \tag{2}$$

where $M_{xy}^*=\mu_{xy}+\delta\mu$ is the new excitonic reduced mass and $M_i^*=m_i^*+\delta m^*$ is the new carrier effective mass. Now we separate the total excitonic wave function $\Phi(\mathbf{r}_e,\mathbf{r}_h)$ into the motion along z and the in-plane motion of the exciton $\phi(\rho)$, $\Phi(\mathbf{r}_e,\mathbf{r}_h)=\Psi(z_e,z_h)\phi(\rho)$, persisting Coulomb effects in the growth direction with the Hamiltonian[6]

0163-1829/95/52(15)/10729(4)/$06.00 ©1995 The American Physical Society

$$H(z_e,z_h)=\sum_{i=e,h}\left[-\frac{\hbar^2}{2M_i^*}\frac{\partial^2}{\partial z_i^2}+V_i(z_i)+\delta E_i\right]+\int_0^\infty d\rho\,\rho\left[\frac{\hbar[\partial_\rho\phi(\rho)]^2}{2M_{xy}^*}-\frac{e^2\phi^2(\rho)}{\epsilon\sqrt{\rho^2+(z_e-z_h)^2}}\right] . \quad (3)$$

This two-variable Hamiltonian can be simplified introducing the factorization $\Psi(z_e,z_h)=\psi(z_e)\psi(z_h)$, and thus, obtaining two Schrödinger equations,[7]

$$\left[-\frac{\hbar^2}{2M_{i,j}^*}\frac{\partial^2}{\partial z_{i,j}^2}+V_{i,j}(z_{i,j})+W_{j,i}(z_{i,j})+\delta E_{i,j}\right]\psi_{i,j}(z_{i,j})=i\hbar\frac{\partial}{\partial t}\psi_{i,j}(z_{i,j}) , \quad (4)$$

where $i=e,j=h$ for the first equation and $j=e,i=h$ in the second equation case. Both equations have to be solved together since the term

$$W_k(z)=\int_{-\infty}^{\infty}dz'\psi_k^2(z')\int_0^\infty d\rho\,\rho\left[\frac{\hbar}{2M_{xy}^*}[\partial_\rho\phi(\rho)]^2-\frac{e^2}{\epsilon\sqrt{\rho^2+(z-z')^2}}\phi^2(\rho)\right] \quad (5)$$

couples ψ_e and ψ_h. To simplify our calculation we have used for the in-plane motion of the exciton the ansatz[7] $\phi(\rho)=(1/a)\exp(-\rho/a)$ where a is the two-dimensional excitonic radius.

Using second-order perturbation theory for the electron-phonon interaction, the contribution to the energy can be written as

$$\delta E=\frac{A}{2\pi}\sum_f\sum_n\int_0^\infty dq_\parallel\frac{q_\parallel|M_{1,f}^n(\mathbf{q}_\parallel)|^2}{\hbar\omega_n(\mathbf{q}_\parallel)+\hbar^2q_\parallel^2/2m_\parallel} \quad (6)$$

and the contribution to the effective mass as

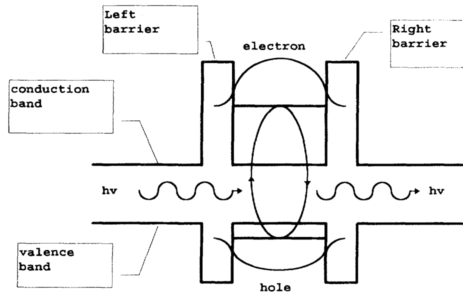

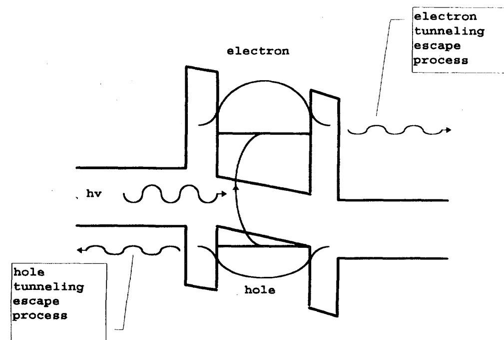

FIG. 1. A schematic illustration of the photoluminescence experiment performed on a double-barrier structure (a) in the absence of an external electric field and (b) with an applied bias.

$$\delta m^*=\frac{A}{2\pi}\sum_f\sum_n\int_0^\infty dq_\parallel\frac{\hbar^2q_\parallel^3|M_{1,f}^n(\mathbf{q}_\parallel)|^2}{[\hbar\omega_n(\mathbf{q}_\parallel)+\hbar^2q_\parallel^2/2m_\parallel]^3} , \quad (7)$$

where the carrier-phonon matrix element is given by[8]

$$M_{1,f}^n(\mathbf{q}_\parallel)=\langle\mathbf{k}_\parallel-\mathbf{q}_\parallel,f,\mathbf{q}_\parallel|H_{i\text{-ph}}|\mathbf{k}_\parallel,1,0\rangle . \quad (8)$$

The matrix element is calculated for the different phonon modes and for the set of intermediate electronic states as the same manner as in Ref. 8. The carrier-phonon interaction is given by

$$H_{i\text{-ph}}=\sum_n\sum_{\mathbf{q}_\parallel}e^{i\mathbf{q}_\parallel\mathbf{r}_\parallel}\Gamma_n(\mathbf{q}_\parallel,z)[a_n(\mathbf{q}_\parallel)+a_n^\dagger(-\mathbf{q}_\parallel)] , \quad (9)$$

where $a_n^\dagger(\mathbf{q}_\parallel)$ $[a_n(\mathbf{q}_\parallel)]$ is the creation (annihilation) operator of an optical phonon with wave vector $\mathbf{q}_\parallel$ and energy $\hbar\omega_n(\mathbf{q}_\parallel)$ in the nth mode and $\Gamma_n(\mathbf{q}_\parallel,z)$ is the coupling function that describes the coupling between an electron (or hole) and the nth optical-phonon mode with frequency $\omega_n(\mathbf{q}_\parallel)$. In a semiconductor quantum well, the phonon modes are modified due to the presence of interfaces. For a single GaAs/AlAs quantum-well structure, there are three significative types of optical-phonon modes that couple to electrons: (a) symmetric-interface-optical-phonon modes with frequencies $\omega_S(\mathbf{q}_\parallel)$, (b) antisymmetric-interface-optical-phonon modes with frequencies $\omega_A(\mathbf{q}_\parallel)$, and (c) the confined phonon modes in the quantum well with frequencies ω_d. The momentum of the confined phonon modes is quantized in the z direction with $q_z=l\pi/d$, $l=1,2,3,\ldots,l_{\max}$ being $l_{\max}=\mathrm{int}(d/a_0)$. The lattice constant of GaAs is $a_0=5.65$ Å and d is the quantum-well width.

The Frölich Hamiltonian for confined modes in a layer of thickness d can be written as[5]

$$\Gamma_n^c(\mathbf{q}_\parallel,z)=\frac{1}{\sqrt{Ad}}\frac{\gamma}{\sqrt{q_\parallel^2+(n\pi/d)^2}}\sin\left[\frac{n\pi}{d}z\right] , \quad (10)$$

where z is growth direction and γ is a coupling constant for GaAs layers.[5]

In the case of interface models, the longitudinal-optical phonon modes consist of one set of antisymmetric modes and one set of symmetric modes.[5] The coupling constant

for the electron-phonon Hamiltonian can be approximated as

$$\Gamma_n^{S(A)}(\mathbf{q}_{\parallel},z)=\left[\frac{\hbar\omega_{S(A)}e^2\beta}{2\varepsilon_0 A}\right]^{1/2}\frac{1}{\sqrt{2q_{\parallel}}}f_{S(A)}(\mathbf{q}_{\parallel},z)\;, \quad (11)$$

where $\hbar\omega_S$ is the energy per phonon ~ 0.0501 eV.[5] The functions f_S and f_A are proportional to the electrostatic potential generated by the phonons and, when z is measured from the center of the GaAs well, is given by

$$f_S(\mathbf{q}_{\parallel},z)=\begin{cases} e^{\mathbf{q}_{\parallel}(z+d/2)}, & z\le -d/2 \\ \cosh(\mathbf{q}_{\parallel}z)/\cosh(\mathbf{q}_{\parallel}d/2), & |z|\le d/2 \\ e^{-\mathbf{q}_{\parallel}(z-d/2)}, & z\ge d/2 \end{cases} \quad (12)$$

in the case of symmetric interface modes. With antisymmetric interface modes, the function f_A is given by[5]

$$f_A(\mathbf{q}_{\parallel},z)=\begin{cases} -e^{\mathbf{q}_{\parallel}(z+d/2)}, & z\le -d/2 \\ \sinh(\mathbf{q}_{\parallel}z)/\sinh(\mathbf{q}_{\parallel}d/2), & |z|\le d/2 \\ e^{-\mathbf{q}_{\parallel}(z-d/2)}, & z\ge d/2\;. \end{cases} \quad (13)$$

Let us discretize time by a superscript n and spatial position by a subscript c and v for the conduction and valence band, respectively. Thus, $\psi_e\to\kappa_c^n$ and $\psi_h\to\kappa_v^n$. The various $z_{e,h}$ values become $c\delta z$ and $v\delta z$ in the conduction and valence bands. To treat the time development we have used a unitary propagation scheme for the evolution operator in both conduction and valence bands obtaining a tridiagonal linear system that is solved by standard numerical method.[7]

Then, Eq. (4) is numerically solved using a spatial mesh size of 0.5 Å and a time mesh size of 1 fs and a finite box (2000 Å) large enough as to neglect border effects. The numerical integration in time allows us to obtain the carrier charge density $Q^{e,h}$ in a defined semiconductor region $[a,b]$ at any time t,

$$Q_{ab}^{e,h}(t)=\int_a^b dz_{e,h}\,|\psi^{e,h}(z_{e,h},t)|^2\;. \quad (14)$$

The decay of the integrated electron charge density, initially trapped in the quantum well, follows essentially the exponential law,[4]

$$Q_{a,b}(t)=Q_0\exp(-t/\tau)\;, \quad (15)$$

where τ is the electron lifetime and Q_0 is a constant. In our case, the $[a,b]$ interval corresponds to the quantum-well limits. So, through numerical integration of Eq. (4) and using Eq. (15), we can obtain the electron and hole lifetimes. In Figs. 2 and 3, we have plotted lifetime versus applied electric field for the different carrier-phonon Hamiltonians. We have used a 100-Å quantum-well width and a barrier thickness of 15 Å in our GaAs/AlAs double-barrier structure. It is clearly shown that the lifetimes are exponentially decreased as we increase the electric field. This effect is due to the field-induced tunneling escape process of the electron-hole pair confined in the quantum-well region. The electron will escape to the right electrode due to its negative charge and, simultaneously, the hole will escape to the left electrode due to its positive sign in the electric charge. Our numerical results plotted in Figs. 2 and 3 may be understood using a semiclassical model. The field-induced tunneling time of a bound carrier through a barrier of height V_0 and d_0 thickness can be written as[4]

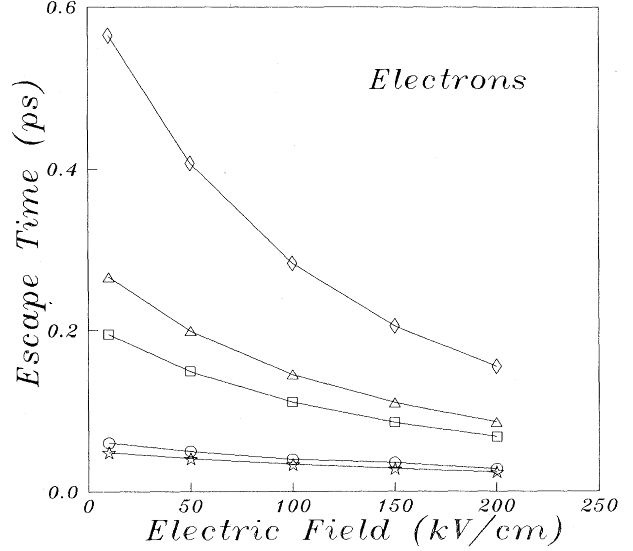

FIG. 2. Electron lifetime vs applied electric field in a 100-Å-wide GaAs/AlAs double-barrier structure. Stars: in the absence of both carrier-phonon and electron-hole interactions. Circles: including Coulomb interaction. Squares: including interface modes and Coulomb interaction in the calculation. Triangles: including confined modes and Coulomb interaction the calculation. Diamonds: including Coulomb interaction and both confined and interface modes in the calculation.

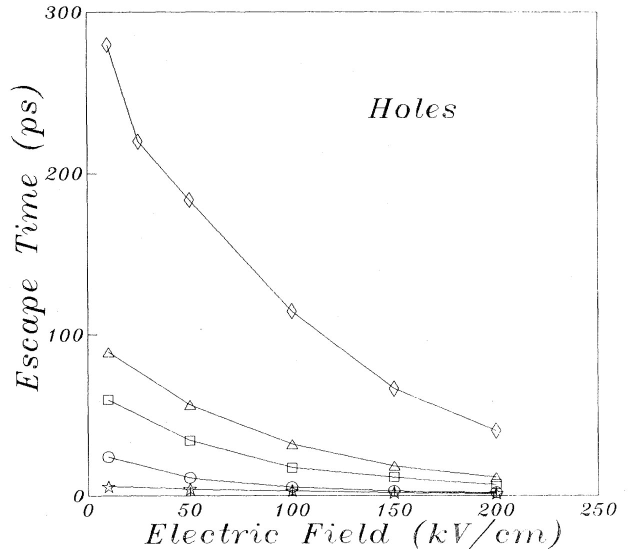

FIG. 3. Hole lifetime vs applied electric field in a 100-Å-wide GaAs/AlAs double-barrier structure. Stars: in the absence of both carrier-phonon and electron-hole interactions. Circles: including Coulomb interaction. Squares: including interface modes and Coulomb interaction in the calculation. Triangles: including confined modes and Coulomb interaction in the calculation. Diamonds: including Coulomb interaction and both confined and interface modes in the calculation.

$$\tau \sim \exp\left\{ \frac{2^{5/2}}{3F\hbar}[(V_0-E)\sqrt{m^*(V_0-E)} + (d_0F - V_0 + E)\sqrt{m^*(V_0-E-d_0F)}] \right\}, \quad (16)$$

where E is the carrier bound energy. In Eq. (16), it is found that the term in the exponential is affected by an F^{-1} coefficient. If we increase F, the electron lifetime is exponentially decreased. In this way, the exponential behavior of the curves plotted in Figs. 2 and 3 is explained. In general, the hole lifetime is higher than the electron lifetime as shown in Figs. 2 and 3. This can be easily explained if we notice that the field-induced tunneling in the valence band is difficult due to the higher hole effective mass. We can clearly notice this effect in Eq. (16) where the exponential factor is affected by a $\sqrt{m^*}$. Increasing the effective mass, the lifetime is also increased.

In Figs. 2 and 3, we have obtained a 20% higher electron and hole lifetime values if the Coulomb potential is included in our calculations. Such an effect is given by the electron-hole interaction.[4] By contrast, the existence of phonon modes in the quantum well increases the carrier lifetime values several times. Such a result can explain in part differences between theory and experiments.[3] In Figs. 2 and 3 we have found that the calculation for both confined and interface modes is important in both cases. Such a numerical result can be easily explained as follows. It is known that the interface modes are important for not too wide and not narrow quantum wells.[8] This is the 100-Å-wide quantum-well case. In addition, we know that the total effective mass can be written as $\delta m^* = \delta m_C^* + \delta m_S^* + \delta m_A^*$ where δm_C^*, δm_S^*, and δm_A^* are the contributions from the confined, symmetric, and antisymmetric carrier-phonon Hamiltonians, respectively. The importance of each phonon mode will increase the corresponding effective-mass value, i.e., δm_C^*, δm_S^*, or δm_A^*. Taking into account Eq. (4), we can notice that the total effective-mass value will determine the dynamics of the carrier wave packet, and thus, the lifetime. From a semiclassical point of view, and using Eq. (16), we can notice that if we increase the effective mass, the obtained tunneling time is also increased. In this way, we will have the corresponding effective-mass contribution in each case obtaining the different electronic lifetimes. Taking this into account, we know that for $d \geq 100$ Å the confined contribution is larger than that of the interface modes.[8] In this way, we can control the role of each phonon mode in the tunneling process varying the quantum-well width.

In summary, in this work we have numerically integrated in space and time the effective-mass Schrödinger equation for an electron-hole pair in a double-barrier structure considering the carrier-phonon interaction. The carrier lifetimes have been obtained at different applied electric fields. Using a semiclassical equation for the tunneling time, the exponential dependence of lifetime with F has been analyzed. The field effect on the localized wave packets has been used to explain the observed lifetimes. Using not too wide and not narrow quantum wells (i.e., $d = 100$ Å), both interface and confined phonon modes are important to study the electron-hole wave-packet dynamics in the double-barrier structure. By contrast, in the wide quantum-well case (i.e., $d > 100$ Å), the confined contribution is larger than that of the interface modes. In such a case, only the contribution of the confined modes will affect the obtained lifetime values. In this way, the carrier-phonon interaction can explain in part the differences between experiments and theoretical models.[3] In addition, varying the quantum-well width, it is possible to control the role of each phonon mode in the obtained carrier lifetime. This effect should be taken into account from a practical point of view in the different Stark-effect-based quantum-well devices.

This work has been supported in part by Gobierno Autónomo de Canarias.

[1]R. Tsu and L. Esaki, Appl. Phys. Lett. **22**, 562 (1973).

[2]L. Esaki, IEEE J. Quantum Electron. **QE-22**, 1611 (1986).

[3]M. Tsuchiya, T. Matsusue, and H. Sakaki, Phys. Rev. Lett. **59**, 2356 (1987).

[4]A. Hernández-Cabrera, P. Aceituno, and H. Cruz, Phys. Lett. A **192**, 269 (1994).

[5]P. J. Turley and S. W. Teitsworth, Phys. Rev. B **44**. 8181 (1991); **50**, 8423 (1994).

[6]R. Zimmermann and D. Bimberg, Phys. Rev. B **47**, 15 789 (1993); J. Phys. (Paris) IV, **3**, 261 (1993).

[7]A. Hernández-Cabrera, P. Aceituno, and H. Cruz, Phys. Rev. B **50**, 8878 (1994).

[8]G. Q. Hai, F. M. Peeters, and T. J. Devreese, Phys. Rev. B **48**, 4666 (1993).